

# Synthesis of Monodisperse, Rodlike Silica Colloids with Tunable Aspect Ratio

Anke Kuijk,\* Alfons van Blaaderen, and Arnout Imhof\*

Soft Condensed Matter, Debye Institute for NanoMaterials Science, Utrecht University, Princetonplein 1, 3584 CC, Utrecht, The Netherlands

**S** Supporting Information

**ABSTRACT:** Although the experimental study of spherical colloids has been extensive, similar studies on rodlike particles are rare because suitable model systems are scarcely available. To fulfill this need, we present the synthesis of monodisperse rodlike silica colloids with tunable dimensions. Rods were produced with diameters of 200 nm and greater and lengths up to 10  $\mu\text{m}$ , resulting in aspect ratios from 1 to  $\sim 25$ . The growth mechanism of these rods involves emulsion droplets inside which silica condensation takes place. Due to an anisotropic supply of reactants, the nucleus grows to one side only, resulting in rod formation. In concentrated dispersions, these rods self-assemble in liquid crystal phases, which can be studied quantitatively on the single particle level in three-dimensional real-space using confocal microscopy. Isotropic, paranematic, and smectic phases were observed for this system.

Dispersions of colloidal rods exhibit various states of orientational and positional ordering, depending on aspect ratio and density. These liquid crystal (LC) phases which are the analogues of molecular LCs have been studied mostly in theory since 1949. Onsager was the first to show that a system of long, hard rods that interact purely through repulsive forces exhibits orientational (nematic) order when the density is increased from the isotropic liquid phase.<sup>1</sup> Later, computer simulations showed that not only nematic but also smectic and crystalline phases can occur in systems of hard spherocylinders, and phase diagrams were calculated as a function of density and aspect ratio.<sup>2–4</sup> The experimental study on the phase behavior of rods has been less extensive. While spherical colloids have proven to be an excellent model system to study the phase behavior of atoms and molecules (especially quantitatively in three-dimensional (3D) real space) similar systems to study rods are rare. Nevertheless, examples of liquid crystal phase behavior have been observed using organic rods (for example fd-virus, TMV, or DNA)<sup>5–7</sup> as well as inorganic materials such as boehmite, vanadium pentoxide, or  $\beta$ -ferric oxyhydroxide.<sup>8–10</sup> The first real space observation of the self-organization of rods into liquid crystal phases has been reported by Maeda in 2003.<sup>11</sup> However, 3D reconstructions of the systems in their work are difficult because of the high refractive index of the materials used. Lower refractive index materials that can be index matched by solvents were used in experimental studies of colloidal spheres and allow quantitative 3D imaging by confocal laser scanning microscopy (CLSM).<sup>12</sup> Examples of such materials are poly(methyl methacrylate) (PMMA) and silica. Ways to fabricate

anisotropic particles from these materials were reported by Keville et al.,<sup>13</sup> Ho et al.,<sup>14</sup> and van Kats et al.<sup>15</sup> The first two described a method to produce PMMA ellipsoids of various aspect ratios by stretching PMMA microspheres embedded in an elastic poly-(dimethylsiloxane) film. Mohraz et al.<sup>16</sup> showed that it is possible to image these particles by CLSM and track their positions and orientations. Although this seems a promising system that shows a nematic phase, no smectic phases were observed for ellipsoidal particles as far as we know. A system of silica rods was developed by van Kats et al.,<sup>15</sup> but the 2D nature of the procedure limits the possibilities of using this system to study significant amounts of concentrated dispersions of rods.

Here we present the wet-chemical synthesis of rodlike silica colloids. This synthesis has a high yield and provides easily enough particles to study concentrated dispersions because of its bulk nature. Moreover, the resulting silica rods allow in situ observation of single particles in concentrated systems. The synthesis was inspired by the work of Zhang et al.,<sup>17</sup> who describe the formation of anisotropic silica nanostructures as being due to gold-induced polyvinylpyrrolidone (PVP) aggregates. Our experiments, however, led to new insights, a modified synthesis, and an alternative model for the growth mechanism of silica rods, which turns out to be unusual for colloid synthesis of anisotropic inorganic particles in solution.

The silica rods were synthesized using a simple one-pot method: ethanol, water, sodium citrate, and ammonia were added to a solution of polyvinylpyrrolidone (PVP) in pentanol (for details and concentrations see Supporting Information). Upon the addition of tetra-ethyl orthosilicate (TEOS), silica rods started to grow. Typical systems are shown in Figure 1. One peculiar aspect of the rods is that one end is flat, while the other end is rounded, i.e. the rods are bullet shaped. The rods generally have a fixed diameter of 200–300 nm and a length varying from 300 nm to 3  $\mu\text{m}$  (aspect ratios from 1 to  $\sim 10$ ), depending on the concentrations of reagents employed. The polydispersity ( $\sigma$ ) of the system could be brought down to 6% in length and 14% in diameter. The refractive index and density of the rods were  $1.45 \pm 0.01$  and  $1.90 \pm 0.03$  g/mL, respectively, corresponding well to the values found for spherical colloidal silica.<sup>18</sup>

There is no straightforward explanation for the growth of anisotropic structures of amorphous materials such as silica. Zhang et al. proposed a templated growth, where PVP molecules form complexes with gold particles and act as soft templates. However, we found that it is not the gold nanoparticles that

**Received:** October 22, 2010

**Published:** January 21, 2011

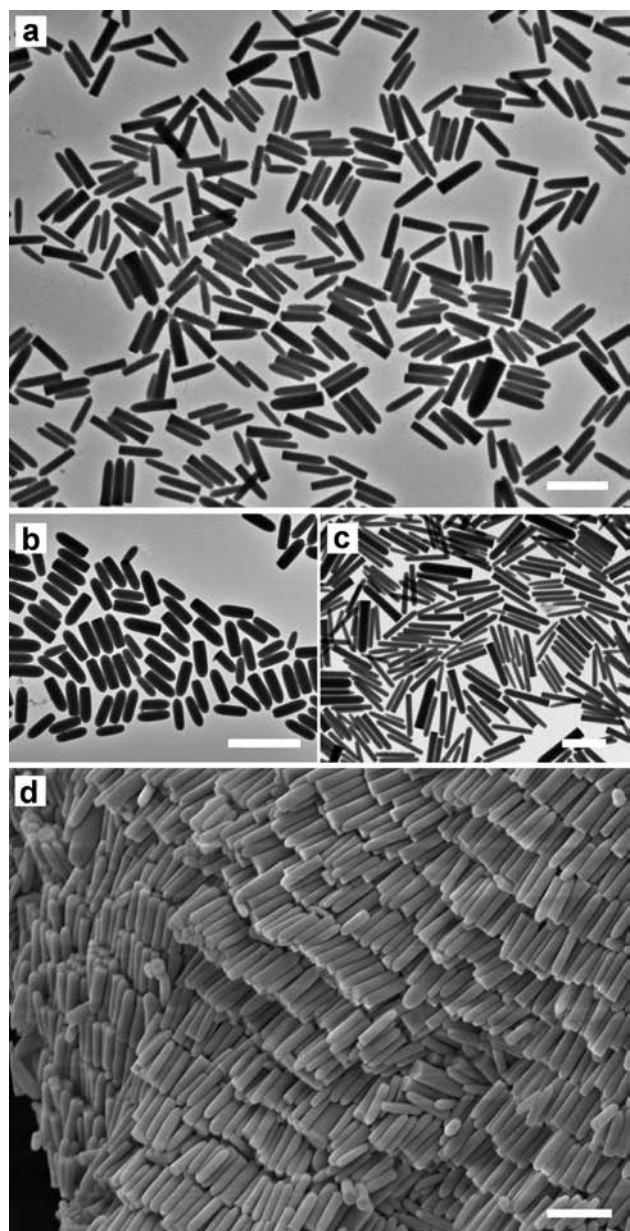


**Figure 1.** Transmission electron microscopy (TEM) images of typical systems after synthesis. (A)  $L/D = 5$  particles ( $\sigma = 6\%$ ,  $14\%$ ). (B)  $L/D = 2.9$  ( $\sigma = 6\%$ ,  $10\%$ ). (C)  $L/D = 7.8$  ( $\sigma = 9\%$ ,  $8\%$ ). (D) Scanning electron microscopy (SEM) image of a highly concentrated dispersion of the rods shown in (A), ordered in a smectic phase. Scale bars are  $2 \mu\text{m}$ .

induce rod formation but the presence of sodium citrate that was used to stabilize the gold particles. The growth mechanism we propose is reminiscent of the vapor–liquid–solid method, where nanowires of several materials grow from metal droplets.<sup>19</sup>

Figure 2 summarizes the growth mechanism: the first step involves the formation of droplets (Figure 2A). Although pentanol, PVP, ethanol, and water mix well for the volume ratios used in this synthesis (no phase separation was observed), a white turbid mixture is formed upon the addition of sodium citrate: an emulsion of water droplets in pentanol stabilized by sodium citrate and PVP. It is striking that this emulsion is stable without a surfactant; addition of a common nonionic surfactant (Igepal CO-520) did not have any noticeable effect on the resulting

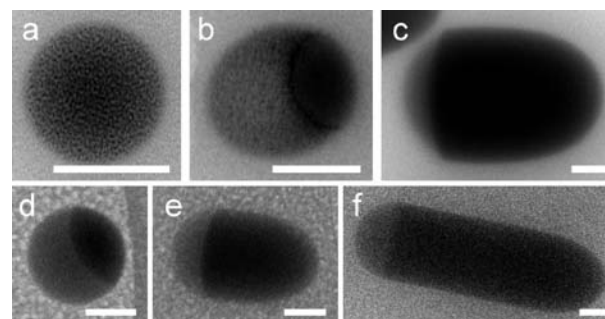


**Figure 2.** (A–C) TEM images of the rods with emulsion droplets attached during growth after respectively 0, 30, and 180 min. (D–F) Cryo-TEM images of rods in a different run after 30, 60, and 120 min, respectively. Scale bars are 100 nm.

emulsion or rod growth. The presence of emulsion droplets was confirmed by dynamic light-scattering measurements on the synthesis mixture containing all reagents except TEOS, where particles with a hydrodynamic radius of 100 nm were found. The diameter of the droplets corresponds to the diameter of the rods after synthesis. The fact that these droplets are visible in the vacuum environment of the electron microscope (Figure 2A–C) suggests that they are not composed of water only but probably contain a high concentration of PVP, which is imaged in the noncryo images. The assumption that the water droplets contain a high concentration of PVP is supported by the observation that, when a large amount of water was added to a solution of PVP in pentanol (water/pentanol = 1:1), the viscosity of the pentanol phase decreased, while the viscosity of the water phase increased, indicating that PVP moved from the pentanol to the water phase. Cryo-TEM images show that the shape and size of the droplet, this time also containing water, was not significantly different from the dried 'droplets' (Figure 2D–F).

The second step in the growth mechanism is initiated by the addition of the silica precursor TEOS. TEOS reacts to silica via a hydrolysis reaction followed by condensation. While TEOS itself dissolves well in pentanol, its hydrolyzed form is hydrophilic and is therefore found inside the water-rich emulsion droplets. The growing silica nucleus is positioned at the surface of the emulsion droplets, as followed from Figure 2B. Subsequently, hydrolyzed TEOS is only supplied from within the droplet and grows onto the existing nucleus rather than nucleating elsewhere. Because of the one-sided supply of new TEOS, the nucleus grows in one direction only (Figure 2C) while the droplet stays attached to one end. Surface tension keeps the angle between the growing silica rod and the emulsion droplet constant, resulting in a nearly constant rod diameter (Figure 3). When all TEOS has reacted to silica, the growth stops. Figure 3 shows that this happens after approximately 17 h of reaction time. The emulsion droplet that is still attached to the rod's end at this point can be washed away, after which a flat rod end remains. Note that this growth mechanism is very different from that of Stöber silica growth which takes place in ethanol–water–ammonia mixtures and where the growth is proportional to the surface area.<sup>20,21</sup>

While the diameter of the rods is fixed by the size of the emulsion droplets, the length and aspect ratio of the rods can be controlled via three different routes: reagent concentrations, seeded growth, or the growth of shells. Alterations in reaction conditions such as temperature and reagent concentrations generally have two possible consequences: either the particles turn out to be longer and eventually curly, or shorter until they

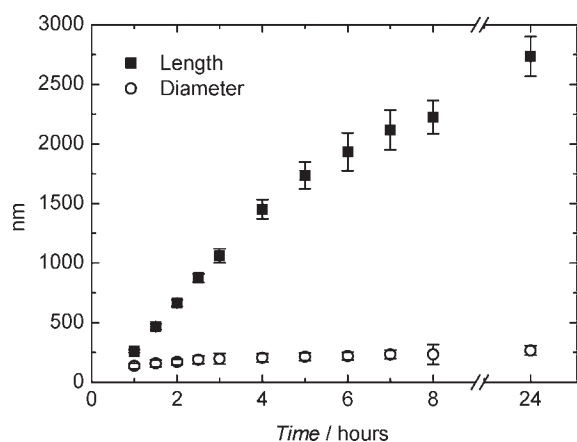


**Figure 3.** Length and diameter of rods during growth followed in time. The growth rate in length was significantly higher than the growth rate in diameter.

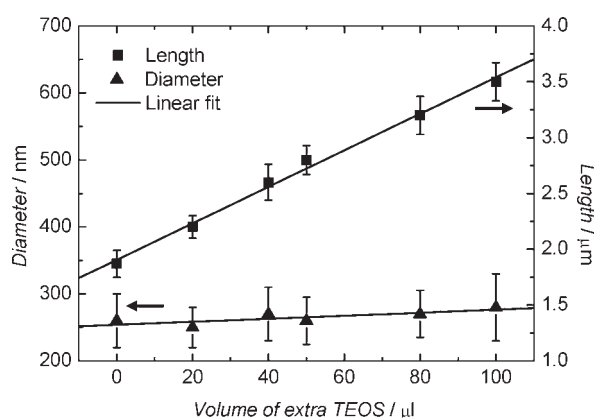


**Figure 4.** Seeded growth of rods after initial synthesis. Length and diameter increase linearly with respect to the volume of extra TEOS that is added, although the increase in length is much larger.

become spherical. The thickness of the rods is hardly affected by concentration changes. Longer particles can be obtained by lowering the water or ammonia concentration. Also, changing solvent to a shorter chain alcohol, adding more ethanol, or increasing the reaction temperature leads to longer rods (for more details see Supporting Information). For shorter particles the opposite of the previously mentioned alterations is applicable. A seeded growth procedure, involving the addition of extra TEOS to the synthesis mixture, allows for growth in length as long as the emulsion droplet is still attached to the rod. This way, the length of the rod can be increased even after the initial synthesis is finished. The volume of extra TEOS that can be added at once is maximally the initial volume used for rod formation and can be added from 6 h after addition of the initial amount. Figure 4 shows that the length of the rods grows linearly with the added amount of TEOS. The diameter of the rods increases only slightly upon extra TEOS addition. Addition of more than the initial volume of TEOS at once leads to unstable rod growth resulting in curly rod-ends. Multiple growth steps are possible and lengths up to  $10\ \mu\text{m}$  were achieved, extending the achievable aspect ratio to  $\sim 25$ . Finally, it is possible to tune the aspect ratio of the rods by growing extra layers of silica around them using standard seeded Stöber or Giesche growth.<sup>20–22</sup>

Growing shells also allows for fluorescent labeling of the rods using the method developed by van Blaaderen.<sup>18</sup> The fluorescently

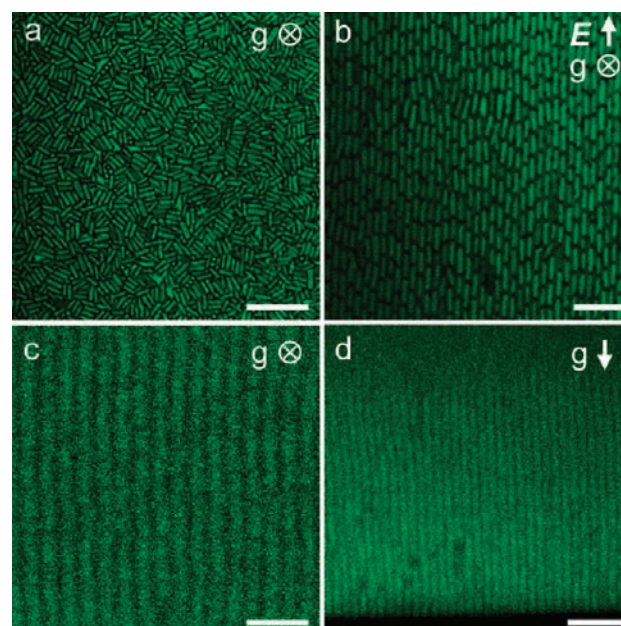


**Figure 5.** Confocal microscopy images of  $L = 2.3\ \mu\text{m}$  ( $\sigma = 10\%$ ),  $D = 640\ \text{nm}$  ( $\sigma = 9\%$ ),  $L/D = 3.6$  rods in isotropic phase (A) and paranematic phase (B) induced by an electric field ( $\sim 0.2\ \text{V}/\mu\text{m}$ ). For  $L = 1.4\ \mu\text{m}$  ( $\sigma = 6\%$ ),  $D = 280\ \text{nm}$  ( $\sigma = 14\%$ ),  $L/D = 5.0$  rods, a smectic phase was observed without applying an electric field. The smectic planes are visible in C, D. Scale bars are  $10\ \mu\text{m}$  (A, D) and  $5\ \mu\text{m}$  (B, C).

labeled rods are suitable for CLSM, which makes 3D imaging possible. Single particle imaging was achieved by creating core–shell particles with a nonfluorescent core, a 30-nm fluorescent inner shell, and a 170-nm nonfluorescent outer shell, as shown in Figure 5A,B. Figure 5A shows that for  $L/D = 3.6$  particles, an isotropic phase is formed when the particles sediment in a 29 vol % dispersion of silica rods in dimethyl sulfoxide. Due to an induced dipole moment, the isotropic phase could be turned into a paranematic phase when an AC electric field of  $0.2\ \text{V}/\mu\text{m}$  (peak-to-peak, 1 MHz frequency)<sup>23</sup> was applied (Figure 5B). In dispersions of higher aspect ratio rods, a smectic phase was observed after sedimentation without an electric field (Figure 5C,D). Until now, the only 3D CLSM measurement of order in colloidal liquid crystals has been that of a nematic phase in a suspension of PMMA ellipsoids.<sup>24</sup> The observation of a smectic phase with CLSM, however, has not been reported before. The ability of our system to form smectic phases as well as isotropic and nematic phases makes it unique and very suitable as a model system for the real-space study of colloidal liquid crystals.

In summary, we developed a new anisotropic monodisperse colloidal model system that is tunable in length and aspect ratio and which allows for real-space 3D observation in highly concentrated dispersions on the single-particle level. Our observation of isotropic, paranematic, and smectic liquid crystal phases shows the potential of these particles as a model system for the quantitative experimental study of rodlike systems and liquid crystal phases in concentrated suspensions.

## ■ ASSOCIATED CONTENT

**S Supporting Information.** Experimental details and influence of concentrations and synthesis conditions on particle dimensions. This material is available free of charge via the Internet at <http://pubs.acs.org>.

## ■ AUTHOR INFORMATION

## Corresponding Author

a.kuijk@uu.nl; a.imhof@uu.nl

## ■ ACKNOWLEDGMENT

J. D. Meeldijk is acknowledged for cryo-TEM measurements.

## ■ REFERENCES

- (1) Onsager, L. *Ann. N.Y. Acad. Sci.* **1949**, *51*, 627.
- (2) Frenkel, D.; Mulder, B. M. *Mol. Phys.* **1985**, *55*, 1171.
- (3) Frenkel, D.; Lekkerkerker, H. N. W.; Stroobants, A. *Nature* **1988**, *332*, 822.
- (4) Bolhuis, P.; Frenkel, D. *J. Chem. Phys.* **1997**, *106*, 666.
- (5) Dogic, Z.; Fraden, S. *Phys. Rev. Lett.* **1997**, *78*, 2417.
- (6) Fraden, S.; Maret, G.; Caspar, D. J. D.; Meyer, R. B. *Phys. Rev. Lett.* **1989**, *63*, 2068.
- (7) Livolant, F.; Bouligand, Y. *J. Phys. (Paris)* **1986**, *47*, 1813.
- (8) Buining, P. A.; Philipse, A. P.; Lekkerkerker, H. N. W. *Langmuir* **1994**, *10*, 2106.
- (9) Pelletier, O.; Davidson, P.; Bourgeaux, C.; Livage, C. *Europhys. Lett.* **1999**, *48*, 53.
- (10) Maeda, H.; Maeda, Y. *Langmuir* **1996**, *12*, 1446.
- (11) Maeda, H.; Maeda, Y. *Phys. Rev. Lett.* **2003**, *90*, 18303.
- (12) van Blaaderen, A.; Wiltzius, P. *Science* **1995**, *270*, 1177.
- (13) Keville, K. M.; Franses, E.; Caruthers, J. M. *J. Colloid. Interface Sci.* **1991**, *144*, 103.
- (14) Ho, C. C.; Keller, A.; Odell, J. A.; Ottewill, R. H. *Colloid Polym. Sci.* **1993**, *271*, 469.
- (15) van Kats, C. M.; Johnson, P. M.; Meerakker, J. E. A. M.; van Blaaderen, A. *Langmuir* **2004**, *20*, 11201.
- (16) Mohraz, A.; Solomon, M. J. *Langmuir* **2005**, *21*, 5298.
- (17) Zhang, J. H.; Liu, H. Y.; Wang, Z. L.; Ming, N. Y. *Chem.—Eur. J.* **2008**, *14*, 4374.
- (18) van Blaaderen, A.; Vrij, A. *Langmuir* **1992**, *8*, 2921.
- (19) Dick, K. A. *Prog. Cryst. Growth Charact. Mater.* **2008**, *54*, 138.
- (20) Stöber, W.; Fink, A.; Bohn, E. *J. Colloid Interface Sci.* **1968**, *26*, 62.
- (21) van Blaaderen, A.; van Geest, J.; Vrij, A. *J. Colloid Interface Sci.* **1992**, *154*, 481.
- (22) Giesche, H. *J. Eur. Ceram. Soc.* **1994**, *14*, 205.
- (23) Yethiraj, A.; van Blaaderen, A. *Nature* **2003**, *421*, 513.
- (24) Mukhija, D.; Solomon, M. J. *Soft Matter* **2010**, *10*, 1039/COSM00493F.